MOLECULAR AND CELLULAR BIOLOGY, Aug. 2006, p. 6005–6015 Vol. 26, No. 16
0270-7306/06/$08.00+0 doi:10.1128/MCB.02067-05

Negative Regulation of Interleukin-2 and p38 Mitogen-Activated Protein Kinase during T-Cell Activation by the Adaptor ALX

Claire E. Perchonock, Melissa C. Fernando, William J. Quinn III, Chau T. Nguyen, Jing Sun, Michael J. Shapiro, and Virginia Smith Shapiro*

Department of Pathology and Laboratory Medicine, University of Pennsylvania School of Medicine, Philadelphia, Pennsylvania 19104

Received 24 October 2005/Returned for modification 19 November 2005/Accepted 3 June 2006

Activation of naïve T cells requires synergistic signals produced by the T-cell receptor (TCR) and by CD28. We previously identified the novel adaptor ALX, which, upon overexpression in Jurkat T cells, inhibited activation of the interleukin-2 (IL-2) promoter by TCR/CD28, suggesting that it is a negative regulator of T-cell activation. To further understand the physiological role of ALX, ALX-deficient mice were generated. Purified T cells from ALX-deficient mice demonstrated increased IL-2 production, CD25 expression, and proliferation in response to TCR/CD28 stimulation. Enhanced IL-2 production and proliferation were also observed when ALX-deficient mice were primed in vivo with ovalbumin-complete Freund's adjuvant and then restimulated ex vivo. Consistent with our initial overexpression studies, these data demonstrate that ALX is a negative regulator of T-cell activation. While TCR/CD28-mediated activations of phosphotyrosine induction, extracellular signal-regulated kinase 1/2, Jun N-terminal protein kinase, IκB kinase α/β, and Akt were unaltered, constitutive activation of p38 mitogen-activated protein kinase and its upstream regulators MKK3/6 were observed for ALX-deficient splenocytes. The phenotype of ALX-deficient mice resembled the phenotype of those deficient in the transmembrane adaptor LAX, and an association between ALX and LAX proteins was demonstrated. These results suggest that ALX, in association with LAX, negatively regulates T-cell activation through inhibition of p38.

The activation of naïve T cells requires two signals, an antigen-driven signal through the T-cell receptor (TCR) and a second antigen-independent costimulatory signal, primarily provided by CD28 in naïve T cells (1). Proximal events in the signaling cascade downstream of the TCR are relatively well understood and include the activation of Src family tyrosine kinases, their phosphorylation of ITAMs within CD3/ζ chains, the recruitment of Syk family kinases, and activation of downstream pathways, including mitogen-activated protein (MAP) kinases, NF-κB, and NFAT (reviewed in reference 13). Costimulation is essential for an effective primary immune response; TCR signals in its absence can result in anergy rather than in activation (26). The outcomes of CD28 signaling include enhanced production of interleukin-2 (IL-2), improved survival, and increased proliferation. This increase in IL-2 protein results from an increase in the transcription of the IL-2 gene as well as in the stability of its mRNA (12, 34). CD28-mediated activation of the IL-2 promoter occurs through the activation of the CD28 response element/AP-1 composite site (RE/AP) (29, 30). However, the details of the signaling downstream of CD28 are less well understood, and further investigation is needed for a greater understanding of the biochemical events required for T-cell activation and immune responses.

We previously cloned and characterized a novel hematopoietic adaptor, ALX, or Adaptor in Lymphocytes of unknown function, X, also known as HSH2 (7, 9, 18). ALX contains a single SH2 domain and contains several potential protein interaction sites, including four PxxP polyproline sequences (7). Previous studies in the Jurkat T-cell line demonstrated that overexpression of ALX inhibited activation of a reporter containing RE/AP, suggesting a role for ALX in TCR/CD28-mediated T-cell activation (7). It was also shown that ALX is itself a target of TCR/CD28 signaling, since it becomes inducibly phosphorylated upon T-cell activation (28). The overexpression studies implicated ALX as a potential negative regulator of T-cell activation, but to confirm this function for ALX in vivo, ALX-deficient mice were generated. Consistent with the results we obtained with Jurkat T cells, ALX-deficient mice had enhanced IL-2 and proliferation in response to CD3/CD28, demonstrating that ALX is a negative regulator of T-cell activation. While no differences in levels of proximal induction of phosphotyrosine, calcium flux, extracellular signal-regulated kinase (ERK), Jun N-terminal kinase (JNK), IκB kinase (IKK), or Akt activation in response to TCR/CD28 stimulation were observed, ALX-deficient splenocytes had constitutively activated p38 MAP kinase that was not further enhanced with TCR/CD28 stimulation. We demonstrate that ALX associates with another negative regulator of T-cell activation, the transmembrane adaptor LAX (40, 41). Therefore, our results indicate that ALX negatively regulates T-cell activation through an association with LAX, leading to inhibition of p38 activation.

* Corresponding author. Mailing address: 288 John Morgan Bldg., Dept. of Pathology and Laboratory Medicine, University of Pennsylvania, 3620 Hamilton Walk, Philadelphia, PA 19104. Phone: (215) 573-9260. Fax: (215) 898-4227. E-mail: shapirov@mail.med.upenn.edu.

MATERIALS AND METHODS

Generation and verification of ALX-deficient mice. A targeting vector was designed to replace exons 2 and 3 of ALX with a neomycin resistance cassette (Fig. 1A). The construct was electroporated in R1 embryonic stem (ES) cells (a

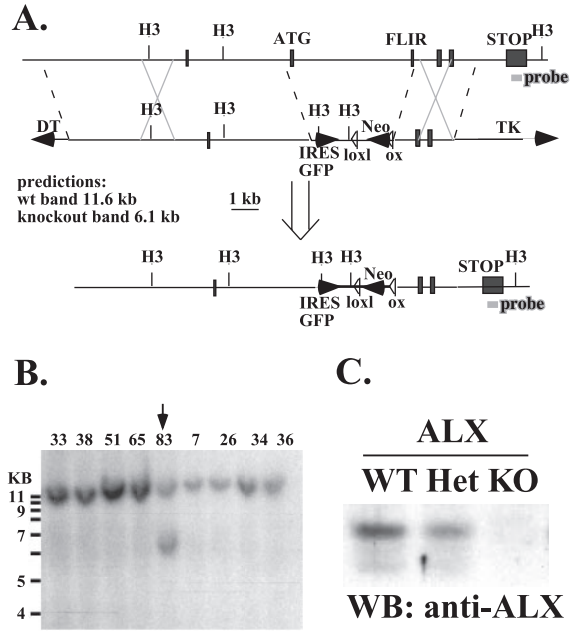

FIG. 1. Generation of ALX-deficient mice via homologous recombination. (A) Schematic of the targeting construct designed to delete exons 2 and 3 via homologous recombination. H3, HindIII; TK, herpes simplex virus thymidine kinase; wt, wild type; IRES, internal ribosome entry site; GFP, green fluorescent protein; DT, diphtheria toxin. (B) Southern blot depicting targeted ES cell clones digested with HindIII and detected with a probe from the last exon of ALX, which is outside of the targeting construct (shown in panel A). All clones had the expected endogenous band (11.6 kb), while clone #83 also possessed a targeted allele (6.1 kb). (C) Western blot (WB) of wild-type (WT), heterozygous (Het), and ALX-deficient (KO) splenocytes probed for expression of ALX protein. Each lane contained lysates from the same number of cell equivalents.

kind gift from Reka Nagy, Andras Nagy, Janet Rossant, and Wanda Abramow-Newerly). After selection with G418 and ganciclovir, DNA from drug-resistant colonies was digested with HindIII and screened by Southern blotting. C57BL/6 blastocysts were injected with a successfully targeted clone. PCR genotyping of tail DNA was employed to identify the genotype of progeny with the following primers: for mALX 15122R, GCT TTT GTT GGT GGA AGG TGA CC; for mALX 14001F, GCC ATC CCC TAT GAT TGC TTG; for mALX KO 14248R, CCA CCC AAG TGT TCC AGC TAG G; and for Neo4, CGT CCA GAT CAT CCT GAT C.

The wild-type allele (1,100 bp) is detected by mALX 15122R plus mALX 14001F.

The knockout allele (900 bp) is detected by mALX KO 14248R plus Neo4.

An antimurine ALX antiserum was generated by immunizing rabbits with a glutathione *S*-transferase fusion protein including the C-terminal portion of ALX (amino acids 182 to 334) (Cocalico Biologicals), and this was used to verify the absence of ALX protein expression in gene-targeted animals. Mice were housed in a specific-pathogen-free facility at the University of Pennsylvania and were used in accordance with the regulations of the university's Institutional Animal Care and Use Committee.

Cell preparation and flow cytometric analysis. Single-cell suspensions of thymocytes were prepared by gently teasing the thymus apart using forceps and then filtering through mesh. Bone marrow lymphocytes were prepared by flushing femurs and tibiae with a 30-gauge needle. Single-cell suspensions of splenocytes were obtained by grinding the organ between glass slides and then passing the material through mesh. Red blood cells were lysed using ACK lysis buffer (Biosource) according to the manufacturer's instructions.

The following fluorescence-activated cell sorter (FACS) reagents were used: B220-allophycocyanin (APC)-Cy7 (eBiosciences), AA4.1-APC (eBiosciences), CD43-fluorescein isothiocyanate (FITC) (Pharmingen), immunoglobulin M (IgM)-biotin (Southern Biotechnology), streptavidin-peridinin chlorophyll *a* protein-Cy5.5 (Pharmingen), CD4-phycoerythrin (PE) (Caltag), CD8-APC (Caltag), CD44-FITC (Pharmingen), CD62L-PE (Pharmingen), CD4-biotin (Pharmingen), CD25-APC (Pharmingen), and CD69-FITC (Pharmingen). Samples were analyzed on a FACSCalibur (Becton Dickinson) or an LSR (Becton Dickinson) instrument. Data were analyzed using FlowJo (Tree Star).

T- and B-cell purification. T cells were isolated by negative selection from whole splenocytes using a SpinSep murine T-cell isolation kit per the manufacturer's instructions (catalog [cat] #17051; Stem Cell Technologies). In brief, splenocytes were incubated with a cocktail of antibodies to label non-T cells. Cells were then incubated with dense particles which bound to the antibody-labeled cells. The mixture was spun over density medium, after which the undesired cells pelleted and the T cells remained at the interface and were collected. This preparation method resulted in approximately 95% pure T cells. Similarly, purified B cells were isolated using either a SpinSep murine B-cell isolation kit (cat #17034; Stem Cell Technologies) or a MACS B-cell isolation kit (cat #130-090-862; Miltenyi Biotec) per the manufacturer's instructions.

B-cell stimulations. Purified B cells were 5-(and 6)-carboxyfluorescein succinimidyl ester (CFSE) labeled and incubated for 3 days with the following stimuli: $F(ab')_2$ goat anti-mouse IgM (final concentration, 10 μg/ml; Jackson Immunoresearch) alone or with anti-CD40 (10 μg/ml; clone HM40-3; Pharmingen), B-lymphocyte stimulator (BLyS) (200 ng/ml; Peprotech), lipopolysaccharide (LPS) (10 μg/ml; K12; Invivogen), or CpG (1 μM; ODN-1826 with a phosphothiolate backbone; Invitrogen).

Cytokine ELISA. Single-cell splenocyte suspensions were plated at a concentration of 1×10^6 cells/ml in 96-well plates precoated with anti-CD3ε (clone 145-2C11; Biolegend) alone or with soluble anti-CD28 added at the time of plating (clone 37.51; Biolegend). Supernatants were collected after 48 h, and concentrations of IL-2 in the supernatants were determined by enzyme-linked immunosorbent assay (ELISA) using a Duoset kit according to the manufacturer's instructions (DY402; R&D Systems). The data were normalized to the amount of IL-2 produced by ALX-deficient mice stimulated with 3 μg/ml plate-bound CD3 and 1 μg/ml CD28. Data are expressed as averages of values for three wild-type and three ALX-deficient mice (F_5 backcrossed) with standard deviations from the mean.

Serum immunoglobulin concentrations. Serum immunoglobulin levels from wild-type and ALX-deficient mice were analyzed by ELISA by using a horseradish peroxidase-based SBA clonotyping system (#5300-05) from Southern Biotechnology Associates according to the manufacturer's instructions.

CFSE proliferation assay. Single-cell suspensions of purified T or B cells were resuspended in 5 ml phosphate-buffered saline (PBS), to which was added 5 ml of PBS containing 0.6 mM CFSE (Molecular Probes). Cells were inverted for 2 min and subsequently quenched with 4 ml fetal bovine serum. The labeled lymphocytes were cultured in RPMI 1640 medium containing 10% fetal bovine serum, L-glutamine, penicillin-streptomycin (all from GIBCO BRL), and 55 μM β-mercaptoethanol for 3 days prior to analysis and either stimulated or not as described in the figure legends. To exclude dead cells, a final concentration of 100 nM TOPRO-3 (Molecular Probes) was added to samples 10 min prior to FACS analysis. A fixed number of 6-μm polystyrene microspheres (Polysciences, Inc.) were added to each sample, and a known fraction of the microspheres was collected by FACS (along with various numbers of cells), permitting the calculation of absolute cell numbers recovered after stimulation. Purified T cells were stimulated with 5 μg/ml plate-bound anti-CD3 (2C11; Biolegend) and 1 μg/ml anti-CD28 (37.51; Biolegend) for 3 days.

Analysis of T-cell signaling in splenocytes. Splenocytes were prepared as described above and resuspended at 100×10^6/ml in PBS. The cells were allowed to rest at 37°C for 20 min prior to stimulation. As indicated in the figures, cells either were left untreated or were incubated for 10 min with phorbol myristate acetate (PMA) (50 ng/ml) or for various times at 37°C with antibodies to murine CD3ε (500A2; Pharmingen) and CD28 (37.51; Biolegend), both at 5 μg/ml. Alternatively, cells were incubated for 30 min at 4°C with anti-CD3 ε (2C11; Biolegend) at 5 μg/ml, washed two times in PBS, and then resuspended in 4°C PBS. Cells were then combined with a fivefold excess volume of 37°C PBS containing anti-hamster secondary antibody (Jackson Immunoresearch) at 10 μg/ml and incubated for various times at 37°C. In this case, samples from unstimulated cells were generated by parallel incubations and washes in the absence of anti-CD3. After stimulation, cells were lysed in detergent at a concentration of 100×10^6/ml of lysis buffer as previously described (7). Samples were analyzed by electrophoresis and Western blotting with the following antibodies (all from Cell Signaling): ERK1/2 (cat #9102), phospho-ERK1/2 (cat #9106), JNK1/2 (cat #9252), phospho-JNK1/2 (cat #9251), AKT (cat #9272), phospho-AKT (S473; cat #9271), phospho-AKT (T308; cat #4056), p38 (cat #9212), phospho-p38 (cat #9216), phospho-IKKα/β (cat #2697), IKKβ (cat #2684), phospho-MKK3/6 (cat #9231), and MKK3 (cat #9232). Antiphosphotyrosine 4G10 was purchased from Upstate Biotechnology.

SEB-mediated Vβ8$^+$ T-cell deletion. Wild-type and ALX-deficient littermates were injected intraperitoneally with 50 μg of staphylococcal enterotoxin B (SEB) (Sigma) in 200 μl of PBS. Mice were bled via retro-orbital puncture on days 0, 2, 4, 8, and 11. Blood lymphocytes were stained with FITC anti-Vβ6 (BD Pharmingen), PE anti-Vβ8 (BD Pharmingen), and APC anti-CD4 (Caltag) to track the percentage of CD4$^+$ Vβ8$^+$ cells over time. CD4$^+$ Vβ6$^+$ cells, which do not respond to SEB, were also examined as a control.

Preparation of blood lymphocytes for flow cytometric analysis. Blood samples (100 to 200 μl) were obtained via retro-orbital puncture and were added to equal volumes of heparin solution (20 units/ml in PBS; Sigma). Blood was lysed in 10 ml of ACK lysis buffer (Biosource) on ice for 10 min and then quenched with 10 ml medium. Cells were spun at 1,200 rpm at 4°C for 8 min and resuspended in 5 ml PBS and filtered through mesh. After spinning, cells were resuspended in FACS buffer.

NP-KLH immunization. Groups of wild-type and ALX-deficient mice were immunized with 100 μg of mouse nitrophenyl-keyhole limpet hemocyanin (NP-KLH) at a conjugation ratio of 30 NP to 1 KLH (Biosearch Technologies) that was precipitated with alum. A booster injection of the same was given on day 47. Mice were sacrificed on day 54. Retro-orbital blood samples were collected on days 0, 7, 14, 21, 28, 35, 47, 50, and 54. Half of each blood sample was allowed to clot to obtain serum, and the other half was used for FACS analysis. Blood lymphocytes were stained with CD4-PE and CD8-PE (Caltag), λ-biotin (Southern Biotechnology), and NP-APC (gift of Jenni Crowley, University of Pennsylvania). The relative representation of CD4$^-$ CD8$^-$ λ$^+$NP-APC$^+$ lymphocytes was determined.

Anti-NP ELISA. Ninety-six-well plates (Nunc) were coated with 5 μg/ml NP-bovine serum albumin (at a 3-to-1 conjugation ratio; Biosearch Technologies) in 0.1 M carbonate buffer overnight at 4°C. Anti-NP IgG (clone BI-8) antibody (a gift from Mark Shlomchik) was used as the standard. Sera from NP-immunized mice were assayed at a 1:100,000 dilution. A secondary horseradish peroxidase-conjugated anti-IgG reagent was used for the detection step (Southern Biotechnology). OptEIA ELISA developer was from BD Pharmingen. Data are expressed as mean concentrations ± standard deviations.

In vivo/ex vivo responses to OVA. Three wild-type and three ALX-deficient mice (3 to 4 months old) were immunized with 100 μg of ovalbumin (OVA; Sigma) plus complete Freund's adjuvant (Fisher). Two weeks later, the mice were sacrificed, and splenocytes of the same genotype were pooled and cultured with OVA to restimulate the cells in vitro. The supernatant from one set of restimulated cells was used for cytokine ELISAs after 48 h, as described above. A second set of restimulated cells was used for a tritiated thymidine incorporation assay to measure proliferation. The standard deviations reflect six wells per condition.

Calcium flux. Single-cell thymocyte suspensions were prepared as described above. Cells were washed and stained in RPMI plus 1% fetal bovine serum. Cells were stained at a concentration of 10×10^6 cells/ml with optimal concentrations of biotinylated anti-CD3 (clone 145-2C11; Pharmingen), biotinylated anti-CD4 (clone RMA 4-4; Pharmingen), Indo-1 (2.6 μg/ml final; Molecular Probes), probenecid (2 mM final; Sigma), and fluorochrome-conjugated anti-CD4 and anti-CD8 (Caltag). Cells were incubated for 30 min at 30°C and then washed twice. Samples were analyzed on an LSR II FACS machine (Becton Dickinson). A baseline reading was collected for 30 s, and then 19 μg/ml streptavidin (Molecular Probes) was added to trigger calcium flux, which was recorded from time 45 s through 5 min 45 s. Ionomycin (5 μl of 10 μg/ml; Sigma) was added for the last 30 s as a positive control.

Coimmunoprecipitation experiments. Expression plasmids for myc-epitope tagged LAX and LAT proteins (41) were kindly provided by Weiguo Zhang (Duke University). The expression plasmids for yellow fluorescent protein (YFP) and for YFP-ALX fusion protein were described previously (7). 293T cells were transfected with either YFP or YFP-ALX expression plasmids combined with either myc-LAX or myc-LAT expression plasmids by use of Fugene6 reagent (Roche Applied Science) according to the manufacturer's instructions (for each combination, 1 μg of each plasmid and 6 μl of Fugene6 were used to transfect cells in one well of a six-well dish). After overnight transfection, cells were lysed in NP-40 buffer and subjected to immunoprecipitation with anti-myc antibody followed by elution with myc peptide as previously described (28). Cell lysates and immunoprecipitates were loaded on gels and analyzed by Western blotting with antibodies to Myc (clone 9B11; Cell Signaling) and to ALX (7).

RESULTS

Generation of ALX-deficient mice. To gain insight into the physiological role of ALX and its potential role in the regulation of IL-2 production, we generated ALX-deficient mice via homologous recombination. The targeting construct was designed to substitute a neomycin resistance cassette for the second exon of ALX, which contains the translational start site, as well as the third exon, including the SH2 domain FLVR motif (Fig. 1A). The FLVR motif within the SH2 domain of ALX is essential for its inhibitory effect on the IL-2 promoter in vitro (28). A successfully targeted clone was identified by the presence of a 6.1-kb band, in contrast to the 11.6-kb wild-type band in a Southern blot (Fig. 1B). C57BL/6 blastocysts were injected with targeted ES cells to generate chimeric mice. ALX-deficient mice were born at the expected Mendelian ratios and were viable, fertile, and grossly normal. Absence of ALX protein was confirmed by Western blotting (Fig. 1C) of

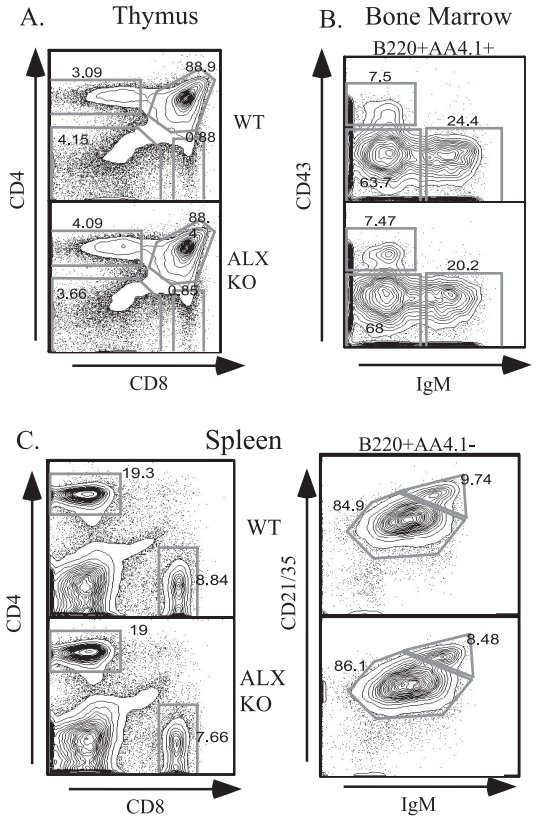

FIG. 2. Unimpaired lymphocyte development in ALX-deficient mice. Wild-type (WT) and ALX-deficient (ALX KO) littermates were analyzed at 8 weeks of age for developmental defects in T- and B-cell development by FACS analysis. (A) CD4$^-$ CD8$^-$, CD4$^+$ CD8$^+$, CD4$^+$, and CD8$^+$ thymocyte populations were similar between wild-type and ALX-deficient mice. (B) Developing B cells in the bone marrow were gated for B220$^+$ AA4.1$^+$ (to exclude recirculating mature B cells) and further subdivided into pro-B-cell (CD43$^+$ IgM$^-$), pre-B-cell (CD43$^-$ IgM$^-$), and immature B-cell (CD43$^-$ IgM$^+$) populations. No differences were observed for any of these populations, demonstrating that B-cell development proceeds normally in ALX-deficient mice. (C) Splenocytes stained with CD4 and CD8 revealed no differences in the proportions of CD4 and CD8 T cells in the periphery. To analyze mature B-cell populations, splenocytes were first gated for B220$^+$ AA4.1$^-$ (to exclude transitional cells) and further subdivided into IgM$^+$ CD21/35$^+$ follicular B cells and IgM^{high} CD21/35^{high} marginal-zone B cells. Again, no differences in the mature B-cell populations in terms of number or proportion were observed for ALX-deficient mice.

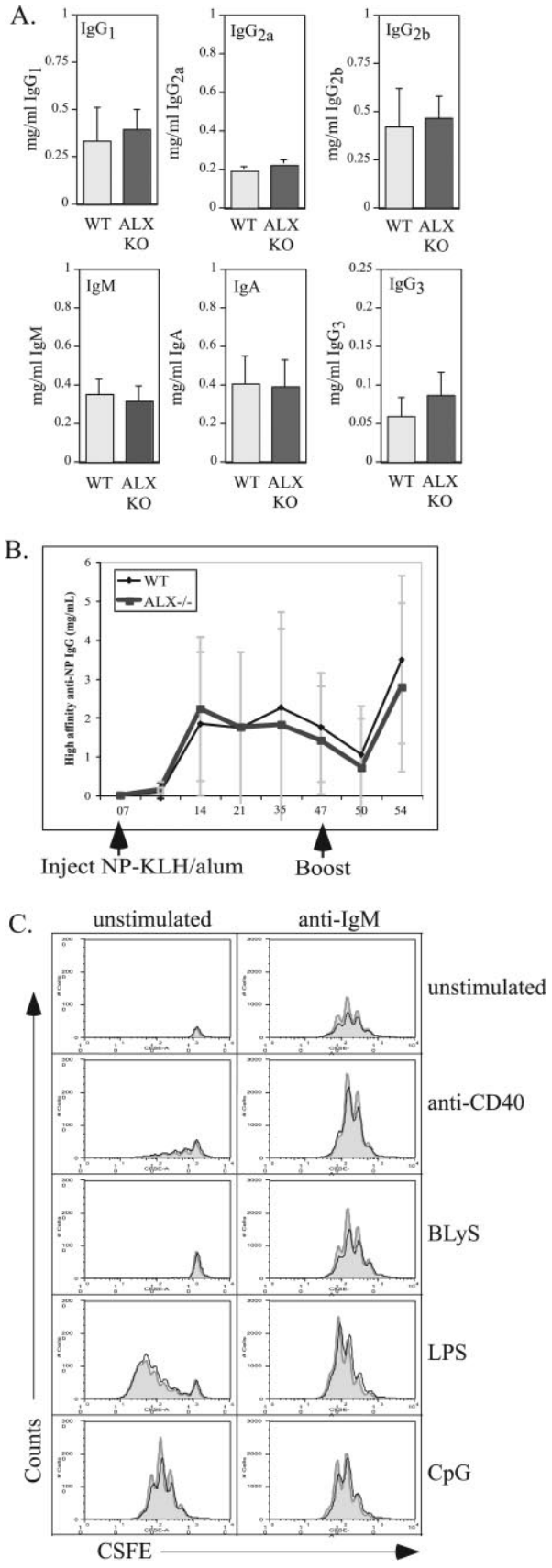

splenocyte lysates using an antiserum to ALX. This antiserum was generated to the C terminus of ALX, outside of the targeting construct, and thus could potentially detect a truncated protein. However, none was detected, demonstrating that ALX-deficient mice lack any ALX protein. In order to reduce potential strain effects, the experiments described herein were performed using mice that had been backcrossed five times to C57BL/6, excluding those done with aged F_1 mice. However, F_1 and F_5 ALX-deficient mice gave similar results (data not shown).

T- and B-cell development proceeds normally in ALX-deficient mice. Since ALX is expressed in both T and B cells, T- and B-cell development in ALX-deficient mice was analyzed by flow cytometric analysis. No significant differences were observed in the total cellularities of thymus and bone marrow (data not shown). The double-negative, double-positive, and CD4 or CD8 single-positive thymocyte populations were normally represented in ALX-deficient mice (Fig. 2A). In the bone marrow, no differences in the pro-B-cell ($B220^+$ $AA4.1^+$ $CD43^+$ IgM^-), pre-B-cell ($B220^+$ $AA4.1^+$ $CD43^-$ IgM^-), and immature B-cell ($B220^+$ $AA4.1^+$ $CD43^-$ IgM^+) populations were observed (Fig. 2B). T and B cells were found in the expected numbers and proportions in peripheral lymphoid organs, such as the spleen (Fig. 2C), lymph nodes, and Peyer's patches (data not shown). Therefore, these data demonstrate that the absence of ALX does not affect lymphocyte development or lymphocyte homing to peripheral lymphoid organs.

Antibody production in ALX-deficient mice. To determine whether ALX-deficient mice exhibited any gross alterations in B-cell function, serum immunoglobulin levels of various isotypes were analyzed. However, no differences between ALX-deficient mice and their wild-type littermates were observed (Fig. 3A). In order to gauge the effectiveness of the immune response to a model antigen in vivo, groups of wild-type and ALX-deficient mice were immunized with NP-KLH. Mice

FIG. 3. Intact T-cell-dependent B-cell responses to antigen in vivo. (A) Serum immunoglobulin levels from wild-type and ALX-deficient mice were analyzed by ELISA. The data represent averages for six wild-type and nine ALX-deficient mice between 12 and 15 weeks of age. The error bars reflect the standard deviations within each group. (B) Five wild-type and four ALX-deficient mice between 9 and 10 weeks of age were immunized with 100 μg alum-precipitated NP-KLH/mouse on day 0, boosted on day 47, and sacrificed on day 54. Sera were collected at the time points shown and were assayed for the concentration of high affinity anti-NP IgG compared to that of the NP-specific IgG1 monoclonal antibody B1-8 used as a standard. The points represent the average concentrations for all wild-type mice or ALX-deficient mice. Error bars reflect the standard deviations within each genotype. (C) Purified B cells from wild-type and ALX-deficient mice were labeled with CSFE and either were left unstimulated or were stimulated with a combination of anti-IgM, anti-CD40, BLyS, CpG, and/or LPS as shown in the figure and as described in Materials and Methods. After 3 days, the cells were analyzed by FACS. TOPRO-3 (100 nM) was added to exclude dead cells from further analysis. A fixed number of 6-μm beads were added to each sample to permit calculation of the absolute number of live cells within each sample. The *y* axis represents absolute numbers of live B cells. For each stimulation condition, the gray-filled histograms represent wild-type B cells and the solid black lines represent ALX-deficient B cells. The results shown are representative of three separate experiments. WT, wild type; ALX KO, ALX deficient.

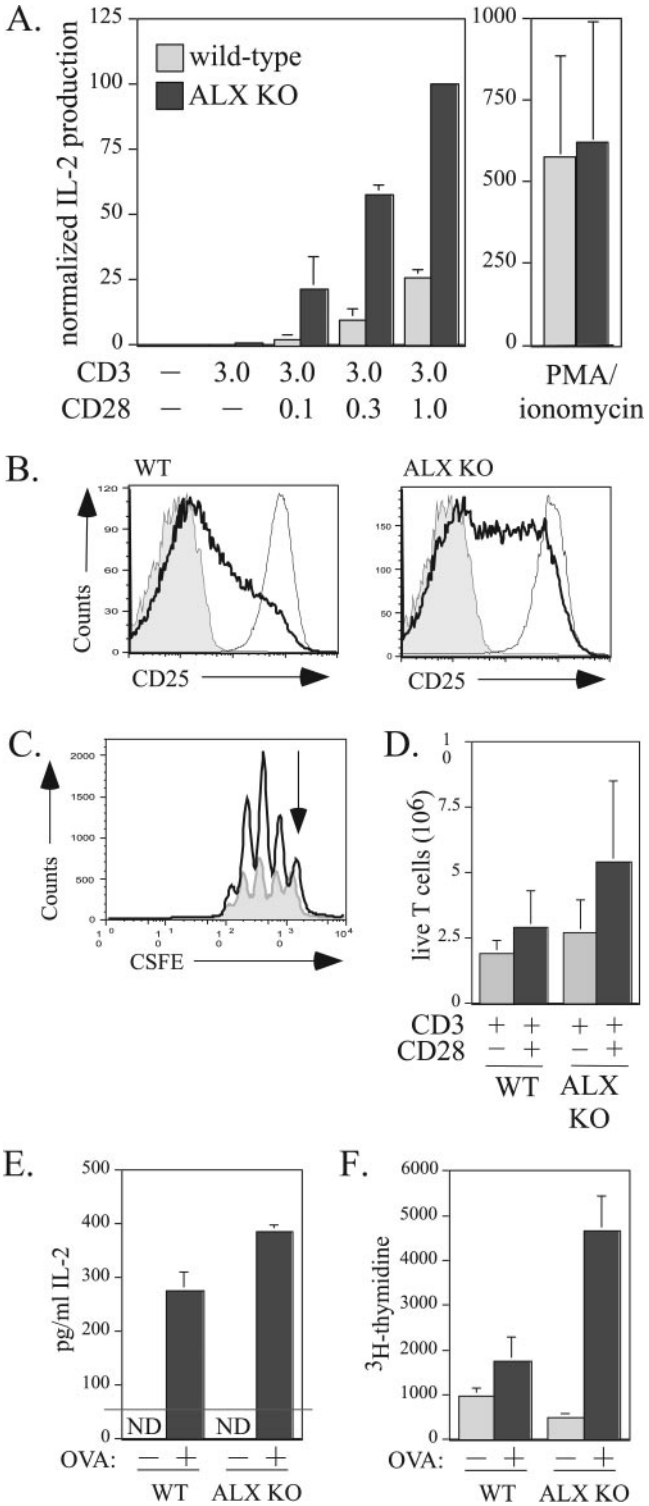

FIG. 4. Increased IL-2 production and T-cell proliferation in ALX-deficient mice. (A) Purified T cells from wild-type and ALX-deficient mice were stimulated with 3 μg/ml plate bound anti-CD3 alone, with 0, 0.1, 0.3, or 1 μg/ml anti-CD28 in solution, or with 50 ng/ml PMA and 1 μM ionomycin as indicated in the figure. Culture supernatants were collected after 48 h and examined for IL-2 production by ELISA. The results shown are averages from three wild-type and three ALX-deficient mice and are normalized to the amount of IL-2 produced by ALX-deficient T cells stimulated with plate-bound anti-CD3 and anti-CD28. Error bars show the standard deviations. (B) Purified T cells from wild-type and ALX-deficient mice either were left unstimulated (shaded area), were stimulated for 48 h with 3 μg/ml plate-bound anti-CD3 with 0.3 μg/ml anti-CD28 in solution (darker line), or were stimulated with 50 ng/ml PMA and 1 μM ionomycin (lighter line) as for panel A and examined for expression of CD25 by FACS. Shown are representative data from four separate experiments. (C) Purified T cells from wild-type (shaded gray) and ALX-deficient (darker line) mice were CFSE labeled and stimulated with plate-bound anti-CD3 with or without anti-CD28. After 3 days, the cells were harvested. TOPRO-3 (100 nM) was added to exclude dead cells from further analysis, along with CD4-PE to analyze proliferation within the T-cell population. A fixed number of 6-μm beads were added to each sample to permit calculation of the absolute number of live cells within each sample. The *y* axis represents absolute numbers of live T cells. The arrow indicates the undivided peak. (D) Quantification of the absolute number of live T cells recovered from four sets of CSFE experiments with wild-type and ALX-deficient purified T cells as described for panel C. Error bars reflect the standard deviations for four mice within each group. (E) Ex vivo hyperresponsiveness to antigen in ALX-deficient mice. Three wild-type and three ALX-deficient mice were immunized with 100 μg of OVA plus complete Freund's adjuvant. After 2 weeks, splenocytes of the same genotype were pooled and cultured ex vivo with 10 μg/ml OVA. Cells restimulated for 48 h were given 1μCi/well [^{3}H]thymidine for an additional 24 h. The supernatant was assessed for IL-2 production by ELISA at 48 hours after OVA restimulation. The standard deviations reflect triplicate ELISA wells. ND, not detected. (F) Results of [^{3}H]thymidine incorporation at 72 h. The standard deviations reflect six wells per condition. WT, wild type; ALX KO, ALX deficient.

were bled weekly and were given a booster injection at day 47. The serum concentrations of high-affinity IgG anti-NP were determined by ELISA. Antibody production kinetics were similar between the wild-type and ALX-deficient groups in both the primary and secondary responses (Fig. 3B). Likewise, no significant difference was observed in the percentages of λ^+NP-binding B cells, as assessed by FACS analysis of peripheral blood (data not shown). To further analyze B-cell function, purified B cells from wild-type and ALX-deficient mice were examined for cell survival and proliferation in vitro in response to stimulation with anti-IgM, anti-CD40, BLyS, LPS, and CpG. During B-cell activation, ALX (HSH2) is upregulated in response to stimuli that promote survival, and its overexpression in WEHI231 can block B-cell antigen receptor-induced apoptosis (9, 10). However, no differences in either proliferation or survival in purified B cells from ALX-deficient mice were observed under any of these conditions (Fig. 3C and data not shown). Taken together, these results indicate that B-cell responses and antibody production are largely unaffected in ALX-deficient mice.

Enhanced IL-2 production and CD25 expression and proliferation in ALX-deficient T cells. Previous work suggested that ALX may act as a negative regulator of T-cell activation, since overexpression in Jurkat T cells inhibited TCR/CD28-induced activation of the IL-2 promoter, specifically at the RE/AP element, which is the main site for TCR/CD28 signal integration (7). However, these studies could not delineate this role for ALX in vivo, since overexpression of an adaptor may alter the stoichiometry of the scaffolded complex, giving a positive regulator in vivo the appearance of a negative regulator when overexpressed. To determine how ALX affects T-cell activation, purified T cells from wild-type and ALX-deficient

mice were stimulated in vitro with anti-CD3 alone or with various concentrations of anti-CD28 for 48 h. As shown in Fig. 4A, ALX-deficient T cells produced more IL-2, as measured by ELISA, than wild-type cells upon CD3/CD28 stimulation, while the amounts of IL-2 produced by the two cell types upon PMA-ionomycin stimulation were similar. Similar results were observed when total splenocytes were stimulated with CD3/CD28 (data not shown). In addition, surface expression of the high-affinity IL-2 receptor alpha chain, CD25, was elevated in ALX-deficient T cells upon CD3/CD28 stimulation, as shown in Fig. 4B. Consistent with increased production of IL-2 and expression of the high-affinity IL-2 receptor, increased proliferation as measured by CSFE was also observed for ALX-deficient purified T cells compared to wild-type T cells (Fig. 4C). Consequently, an increased absolute number of live cells was found in the ALX-deficient compared to wild-type purified T-cell cultures after either anti-CD3 or anti-CD3/CD28 stimulation (Fig. 4D). To test whether the observed enhancement of proliferation and IL-2 production would also be seen after priming in vivo with antigen, wild-type and ALX-deficient mice were immunized with OVA, and their splenocytes were restimulated ex vivo with OVA 2 weeks later. ALX-deficient splenocytes showed a statistically significant increase in IL-2 production at 48 h postrestimulation (Fig. 4E). To measure proliferation, [^{3}H]thymidine was added to cultures for the last 24 h of the 72-h ex vivo restimulation period. Wild-type splenocytes demonstrated a twofold increase in proliferation upon OVA restimulation (Fig. 4F). In contrast, ALX-deficient splenocytes showed a 10-fold increase in [^{3}H]thymidine incorporation over baseline upon OVA restimulation (Fig. 4F). Consistent with our previous in vitro results obtained by use of anti-TCR/CD28 stimuli, in vivo antigen-primed ALX-deficient T cells showed increased IL-2 production and proliferation. Taken together, the enhanced IL-2 production and proliferation in ALX-deficient cells demonstrate that ALX is a negative regulator of T-cell activation, in agreement with our previous overexpression studies with Jurkat T cells.

Equivalent levels of activation-induced cell death in response to superantigen. While the increase in proliferation in ALX-deficient T cells is most likely due to increased IL-2 production and CD25 expression, it was also possible that a defect in activation-induced cell death could have also contributed to the differences observed between wild-type and ALX-deficient mice. To test this possibility, we examined Vβ8$^+$ T-cell survival in response to SEB. SEB is a superantigen which polyclonally activates T cells according to their Vβ usage; in this case, SEB stimulates TCRs containing Vβ8 but not those containing Vβ6. Persistent SEB stimulation results in selective depletion of responding T cells by activation-induced cell death. Wild-type and ALX-deficient littermates were treated with SEB, and the percentages of CD4$^+$ Vβ8$^+$ cells in the blood were measured over time by FACS. Similar kinetics and extents of SEB-induced depletion CD4$^+$ Vβ8$^+$ cells were observed for the wild-type and knockout groups (Fig. 5A). As expected, CD4$^+$ Vβ6$^+$ cells remained unaffected (Fig. 5B). Therefore, ALX-deficient mice deleted CD4$^+$ Vβ8$^+$ T cells to the same extent that wild-type mice did; activation-induced cell death in this context is unaltered.

Splenomegaly and increased T-cell activation in aged ALX-deficient mice. Mice with altered sensitivity to T-cell activation may develop autoimmunity. In order to investigate whether ALX deficiency leads to spontaneous pathology in older mice, a cohort of wild-type and ALX-deficient mice (F_1 backcross) were allowed to age and were sacrificed for analysis at 15 to 16 months. Many ALX-deficient mice had mild splenomegaly, with 4 (of 15) having spleen weights three times greater than expected; 2 of these had approximately 10-fold increases in spleen size (Fig. 6A). FACS profiling demonstrated that although spleens were enlarged in ALX-deficient mice, populations of granulocytes, T cells (both CD4 and CD8), and B cells were present in the expected proportions (data not shown). Therefore, the size increase was not due to a disproportionate increase within a single population but was due to a general increase in cellularity across populations (Fig. 6B). At this age, most T cells from the wild-type mice were memory cells, which prevented a quantitative comparison between wild-type and ALX-deficient mice. However, differences were observed in the levels of expression of the activation marker CD69. Both CD4$^+$ and CD8$^+$ T cells from ALX-deficient mice had increased CD69 expression compared to the corresponding levels for wild-type mice, demonstrating increased activation within these populations (Fig. 6C). The presence of splenomegaly and the increased expression of activation markers suggested the possibility that these mice had developed autoimmune disease. However, upon examination, no glomerulonephritis or immune complex deposition was found in the kidneys of older ALX-deficient animals (data not shown). Rather, these data suggest that in the absence of ALX, mice accumulate activated T cells with age, which may predispose them to the development of autoimmune disease when challenged in an appropriate model. This possibility will be examined when backcrossing to C57BL/6 to 10 generations has been completed.

Constitutive activation of p38 MAP kinase pathway in ALX-deficient splenocytes. To determine the biochemical cause for the increased IL-2 production and CD25 expression observed for ALX-deficient T cells, we examined the signaling pathways activated downstream of TCR/CD28. As a control, lysates were blotted with antibodies to ALX. As expected, the appropriate band was absent for extracts from ALX-deficient cells (Fig. 7A). Similar to our previous results with Jurkat T cells, stimulation by anti-CD3/CD28 induced a shift in ALX mobility within 5 min in wild-type splenocytes. The complete shift with PMA stimulation is presumably due to a shift in ALX mobility in all splenocytes expressing ALX rather than only in T cells stimulated by TCR/CD28. This result further demonstrates that ALX is a target downstream of TCR and CD28 during T-cell activation and implicates it as a proximal negative regulator of T-cell activation. Initial examination of phosphotyrosine induction or calcium flux in response to CD3 cross-linking did not demonstrate any differences between wild-type and ALX-deficient cells in either the rate or extent of induction or downregulation (Fig. 7A and B). To further analyze individual signaling pathways downstream of the TCR and CD28, phospho-specific antibodies were used to probe extracts of wild-type or ALX-deficient splenocytes stimulated over a 45-minute time course. For each phospho-specific antibody, controls examining the total level of each signaling molecule were used for comparison. PMA stimulation was used as a positive control, since it bypasses many proximal signaling

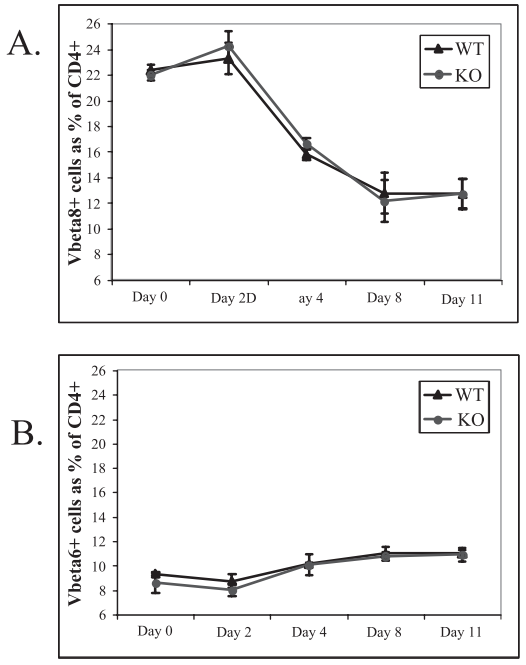

FIG. 5. Unaffected Vβ8$^+$ T-cell deletion in response to SEB immunization. (A) Three wild-type and three ALX-deficient littermates were injected intraperitoneally with 50 μg SEB in 200 μl PBS. At the various time points postinjection shown in the figure, blood was collected and examined by flow cytometry to determine the relative representations of Vβ8$^+$ T cells (A) and Vβ6$^+$ T cells (B), expressed as a percentage of total CD4$^+$ cells. The black triangles represent the average of each population from three wild-type mice at each time point, while the gray circles represent the average of each population from ALX-deficient mice. Error bars reflect the standard deviations. WT, wild type; KO, ALX deficient.

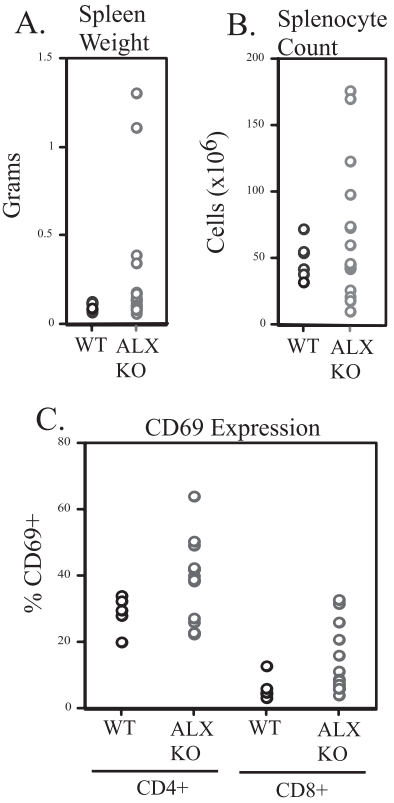

FIG. 6. Aged ALX-deficient mice show enhanced splenic size and T-cell activation. Six wild-type and 15 ALX-deficient F_1 129/B6 mice were allowed to reach ages of 15 to 16 months, and then they were examined for abnormalities in peripheral lymphoid organs and pathology. (A) Spleens were isolated from each animal and their weights were recorded. Shown is a scatterplot for all mice demonstrating that while older wild-type mice had normal spleen weights of approximately 0.1 g, significant variation in spleen size was observed in older ALX-deficient animals. (B) The spleens whose weights are shown in panel A were examined for total cellularity. Data are shown as a scatterplot with each point representing cellularity in millions of cells. (C) Splenocyte suspensions from older animals were stained with various cell surface molecules to examine the activation status (by CD69 expression) on CD4$^+$ and CD8$^+$ T cells by flow cytometry. Shown is the percentage of CD69$^+$ cells from each animal in a scatterplot within either the CD4$^+$ or CD8$^+$ populations. WT, wild type; KO, ALX deficient.

events downstream of TCR and CD28 during T-cell activation. No significant differences in the extents or kinetics of phosphorylation of ERK1/2, JNK1/2, Akt (at both regulatory sites T308 and S473), or IKKα/β were observed between wild-type and ALX-deficient mice (Fig. 7C). However, in contrast to wild-type splenocytes, which have a low basal level of p38 MAP kinase activation and show substantial activation when induced by TCR/CD28 or PMA stimulation, ALX-deficient splenocytes exhibited constitutive phosphorylation of p38 which was not further increased upon stimulation with TCR/CD28. p38 MAP kinase activation can be mediated by phosphorylation at a regulatory TGY motif by the MAP kinase kinases MKK3/6. To determine whether constitutive p38 activation was due to constitutive activation of MKK3/6, we utilized phospho-specific antibodies to MKK3/6 (Fig. 7D). As was observed for p38 activation, ALX-deficient mice had constitutive activation of MKK3/6, which was not enhanced by either TCR/CD28 or PMA stimulation. Therefore, p38 activation in ALX-deficient mice is mediated by constitutive activation of its upstream MAP kinase kinases, MKK3/6.

ALX associates with the transmembrane adaptor LAX but not LAT. To understand the molecular mechanisms by which ALX acts as a negative regulator of T-cell activation, the protein(s) with which ALX associates must be identified. Mice deficient in proteins that are involved in the same pathway as ALX should have a similar phenotype (normal T-cell development, enhanced IL-2 production, enhanced proliferation, and enhanced activation of p38 MAP kinase). Interestingly, mice deficient in the negative regulator LAX were recently described, and their phenotype is similar to that observed for ALX-deficient mice (40, 41). These similarities suggested that ALX and LAX may function in the same pathway and may directly associate. To test this, 293T cells were transfected with an expression construct for ALX in addition to either vector control, myc-tagged LAX, or myc-tagged LAT. LAT is a transmembrane adaptor related to LAX but is a positive regulator of TCR signaling, being necessary for T-cell development and activation (6, 39). As shown in Fig. 8, LAX coprecipitated with ALX. Although LAT was expressed at a level higher than that for LAX, no association with ALX was observed. Therefore, our data support a model where ALX is a negative regulator of

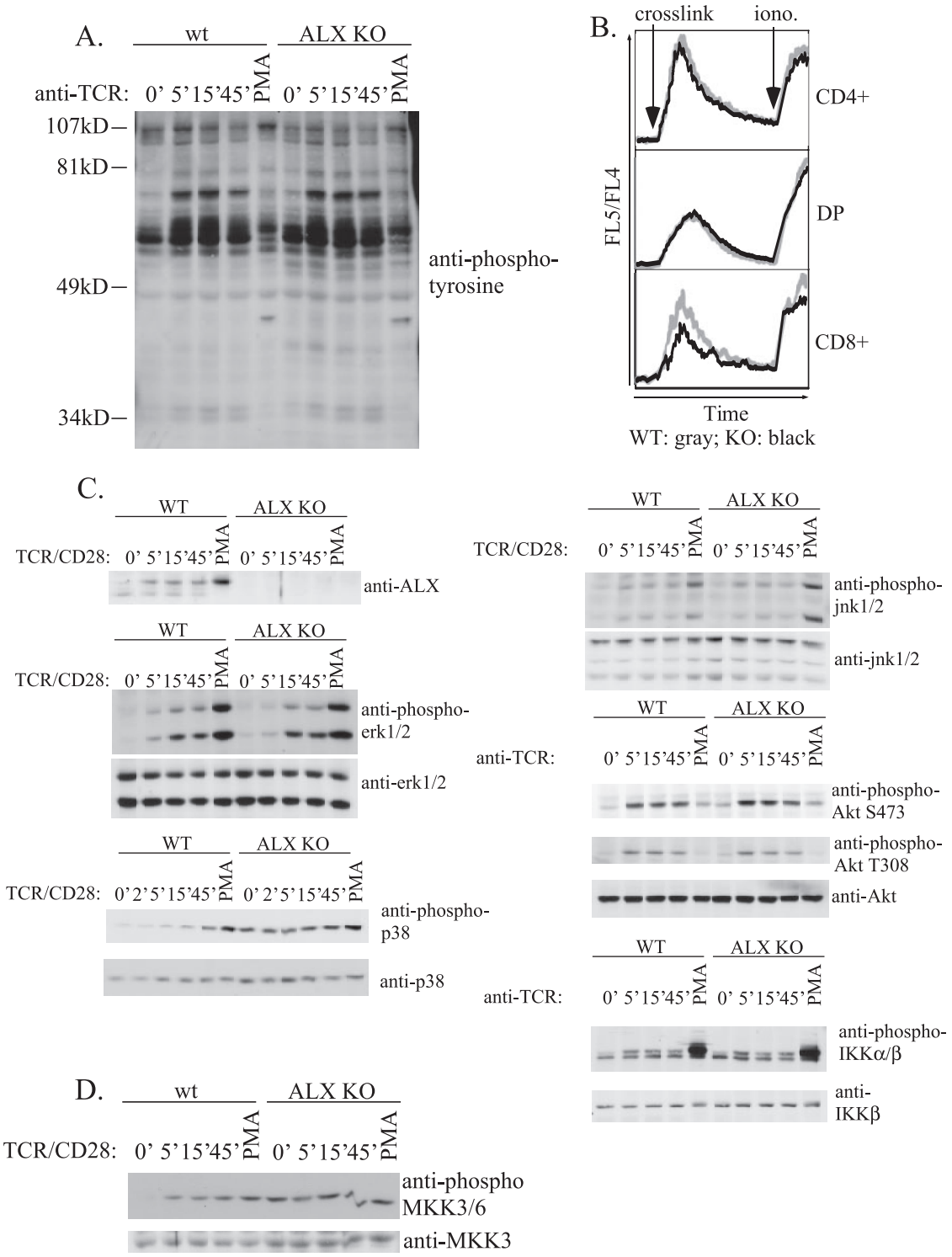

FIG. 7. Analysis of T-cell signaling in primary wild-type and ALX-deficient splenocytes. (A) Splenocytes from either wild-type or ALX-deficient mice were harvested and resuspended at 100×10^6 cells/ml in PBS, stimulated with cross-linked anti-CD3 (2C11) as described in Materials and Methods, and examined for total phosphotyrosine by Western blotting with 4G10. (B) Thymocytes from either wild-type or ALX-deficient mice were examined for their abilities to flux calcium in response to CD3 cross-linking by FACS analysis. Arrows indicate the times at which streptavidin cross-linker (crosslink) and ionomycin (iono.) were added to each sample. Calcium flux is shown for $CD4^+$ (top panel), $CD4^+$ $CD8^+$ double-positive (DP) (middle panel), and $CD8^+$ single-positive (bottom panel) thymocytes. WT and KO lines show the calcium flux in the indicated types of thymocytes. Shown are representative data from three independent experiments. (C and D) Splenocytes from wild-type and ALX-deficient mice were stimulated as described in Materials and Methods with either CD3 or CD3/CD28 over a 45-min time course to examine the phosphorylation status of various signaling intermediates during T-cell activation. PMA was used as a positive control. Within each set, parallel blots were generated by utilizing the same stimulated samples to examine phosphorylated as well as total protein expression. WT, wild type; KO, ALX deficient.

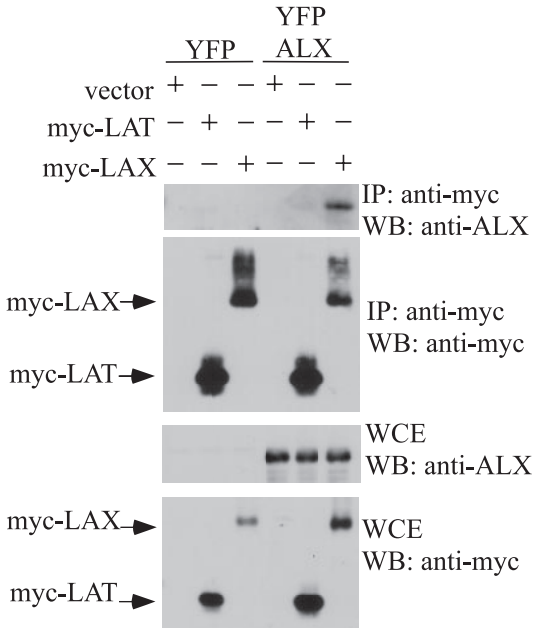

FIG. 8. Association of ALX with the transmembrane adaptor LAX. Expression plasmids for myc-tagged LAT and LAX were cotransfected into 293T cells with YFP-tagged ALX along with the appropriate vector controls. The following day, cells were lysed in NP-40 lysis buffer and immunoprecipitated (IP) with anti-myc antibody, and the immunoprecipitated complexes were eluted from the protein A beads with an excess of myc peptide. Whole-cell lysates and immunoprecipitates were then examined by Western blotting (WB) with antibodies recognizing the myc tag or with antibodies to ALX. WCE, whole-cell extract.

T-cell activation which functions through LAX leading to p38 MAP kinase.

DISCUSSION

Our previous work with Jurkat T cells suggested that ALX may act as a negative regulator of T-cell activation, since ALX overexpression inhibited the activation of the IL-2 promoter as well as that of the RE/AP composite element in response to TCR/CD28 stimulation. However, since the function of an adaptor is to bring together two or more proteins in a complex, a positive regulator may act like a negative regulator when overexpressed in vitro if the stoichiometry of the signaling complex is compromised. Therefore, to understand the physiological role of ALX in T-cell activation, ALX-deficient mice were generated and examined. Consistent with our results with Jurkat T cells that ALX functions as a negative regulator, purified T cells from ALX-deficient mice produced more IL-2, expressed greater levels of CD25, and proliferated more in response to TCR/CD28 stimulation than wild-type controls. In addition, these increases in IL-2 and proliferation were observed when ALX-deficient mice were challenged with OVA-complete Freund's adjuvant in vivo and reexamined for OVA responses ex vivo. To determine the mechanism of this activation in ALX-deficient mice, signaling pathways in T cells were examined. While levels of tyrosine phosphorylation, calcium flux, and activation of the Akt, IKKα/β, ERK1/2, and JNK1/2 pathways in response to TCR/CD28 were comparable between wild-type and ALX-deficient mice, the p38 MAP kinase pathway was constitutively activated in ALX-deficient mice. Similarly, the upstream regulatory MAP kinase kinases, MKK3/6, were also found to be constitutively activated in ALX-deficient mice, demonstrating that ALX is a negative regulator of T-cell activation and of p38 MAP kinase activation specifically.

To understand further the molecular mechanisms of p38 regulation by ALX, we searched for other proteins potentially involved in the same pathway, as suggested by the fact that their deficiency resulted in a phenotype reminiscent of that of ALX-deficient mice (namely, normal T- and B-cell development, enhanced IL-2 and proliferation in response to T-cell activation, and enhanced p38 MAP kinase activation). By use of these criteria, the transmembrane adaptor LAX was identified (40, 41). ALX and LAX interact directly in 293T cells, under conditions where no association between ALX and a related transmembrane adaptor, LAT, is observed. Therefore, our results demonstrate that ALX is a negative regulator of T-cell activation and p38 MAP kinase activation possibly mediated through an association with the transmembrane adaptor LAX. While there are similarities in the phenotypes of LAX- and ALX-deficient mice, LAX-deficient T cells also show enhanced calcium flux and Akt activation in response to TCR stimulation, unlike those of ALX-deficient mice (40). Since the ALX phenotype is a subset of the phenotype observed for LAX-deficient mice, we propose that ALX functions downstream of LAX to negatively regulate p38 MAP kinase activation.

The role of p38 MAP kinase in the regulation of IL-2 during T-cell activation was first demonstrated using the inhibitor SB203580, which blocks induction of IL-2 in both human and murine T cells in response to CD3/CD28 stimulation (35, 38). A detailed mapping of the primary site of effect of SB203580 within the IL-2 promoter demonstrated that activation of RE/AP, but not of AP-1 or NF-κB, was inhibited (31). Similarly, overexpression of p38 was found to enhance activation of RE/AP (31). Our results are consistent with this previous work, since ALX deficiency results in constitutive p38 MAP kinase activation and enhanced IL-2 production, while ALX overexpression in Jurkat T cells inhibits activation of RE/AP and the IL-2 promoter (7). In addition, both the IL-2 and CD25 promoters are regulated by NFAT, which is a target of p38 MAP kinase activation (11, 25, 36). It should be noted that T-cell activation was not perturbed in T cells deficient in p38α (14). However, the importance of p38 in vivo might not have been revealed in this study because there are two other isoforms of p38 expressed in T cells, p38β and p38δ, and these may have overlapping functions (8, 35). The in vivo role of p38 MAP kinases in T-cell activation may be revealed only when multiple isoforms are deleted.

Expression of IL-2 is upregulated through both an increase in transcription from the IL-2 promoter/enhancer during T-cell activation and an increase in its mRNA stability (34). Both JNK and p38 MAP kinases have been shown to play a role in regulating mRNA stability in different systems (reviewed in reference 5). However, the stability of the IL-2 mRNA has been found to be dependent solely on JNK activation (2). Further, constitutive activation of the p38 MAP kinase pathway was not found to alter IL-2 mRNA stability (2). In ALX-deficient mice, no alterations in the activation of JNK were

observed in response to TCR/CD28 stimulation. Therefore, the increase in IL-2 in ALX-deficient mice is unlikely to result from increased IL-2 mRNA stability but rather from increased transcription.

T cells have two pathways leading to p38 MAP kinase activation. The "classical" pathway of p38 activation arises from phosphorylation by an upstream MAP kinase kinase (MKK3 or 6), which is itself regulated by phosphorylation by a MAP kinase kinase kinase (reviewed in references 4 and 21). Recently, an "alternative" pathway, in which tyrosine phosphorylation of p38 at Y323 leads to autophosphorylation at the regulatory TxY motif, leading in turn to activation, was described (24). This alternative pathway is not dependent upon MKK3 or MKK6 but is dependent on ZAP-70, which either directly phosphorylates p38 or activates a downstream tyrosine kinase which then phosphorylates p38 at Y323 (24). ALX-deficient mice have constitutive activation of MKK3/6 as well as p38 MAP kinase, demonstrating that the classical pathway leading to p38 MAP kinase activation is constitutively activated. It remains possible that the alternative pathway is also activated in ALX-deficient mice; this possibility will be examined in the future.

The alternative pathway has been found to be negatively regulated by GADD45α, since GADD45α-deficient mice have constitutive activation of p38 MAP kinase through the alternative pathway (23). GADD45α was originally identified as negative regulator of T-cell activation, since splenocytes from GADD45α-deficient mice proliferated more in response to CD3 stimulation than wild-type splenocytes (22). Splenocytes from GADD45α-deficient mice and wild-type mice proliferated identically when grown in the presence of exogenous IL-2, implying that differences in proliferation may be caused by differences in IL-2 production. However, this possibility was not examined explicitly. As GADD45α-deficient mice age, they develop a lupus-like autoimmune syndrome, characterized by the presence of autoantibodies, proteinuria, and glomerulonephritis (22). ALX-deficient animals also have enhanced proliferative responses to T-cell activation. Although they do not develop an overt autoimmune syndrome, older ALX-deficient mice exhibit splenomegaly and an increased frequency of activated T cells (by CD69 expression), indicating that they may be poised to develop autoimmunity. This will be tested explicitly in autoimmune models once backcrossing is completed, to avoid potential complications arising from mixed genetic backgrounds.

Transgenic mice have also been generated with a constitutively activated MKK6 [MKK6(Glu)] under the control of the distal lck promoter, which resulted in constitutive activation of p38 in thymocytes and peripheral T cells (20). The primary phenotype in these mice is increased production of gamma interferon (IFN-γ) in previously polarized Th1 cells. We did not observe any difference in IFN-γ production in ALX-deficient mice when naïve splenocytes were stimulated for 48 h with CD3/CD28 (data not shown). However, naïve splenocytes from MKK6(Glu) transgenic mice had a level of IFN-γ production similar to that of wild-type mice after 2 days of stimulation with concanavalin A and IL-12 (20). Preliminary data have not shown any defects in Th1 or Th2 polarization in ALX-deficient mice (data not shown), and further work is required to determine whether there are functional defects in previously polarized cells from ALX-deficient mice.

It is clear from other studies that p38 MAP kinase plays a role in both positive and negative selection of thymocytes (17, 33). Our preliminary results do not demonstrate any gross aberrations in T-cell development in ALX-deficient mice, based on absolute numbers or proportions of CD4/CD8 double-negative, double-positive, or single-positive cells. However, it is possible that alterations in T-cell development may not become apparent until these mice are interbred with a T-cell receptor transgenic line, a possibility which is under investigation.

ALX is structurally similar to the lymphocyte-specific adaptor RIBP/TSAd (3, 19, 32, 37), which also acts as a negative regulator of IL-2 promoter activation when overexpressed in vitro. Based on this similarity, we proposed that ALX and RIBP/TSAd might have redundant functions (7). However, ALX-deficient mice have a phenotype that contrasts with that reported for RIBP/TSAd-deficient mice. Whereas RIBP-deficient mice have a mild decrease in IL-2 production and proliferation in response to CD3/CD28 stimulation (19), ALX-deficient mice have enhanced IL-2 and proliferative responses. Recent work has demonstrated that under suboptimal stimulation conditions, RIBP/TSAd-deficient mice have proximal signaling defects, emphasizing the role of this adaptor as a positive regulator of T-cell activation (15). Therefore, it does not appear that these two related adaptors act redundantly; rather, they may have opposing functions. Furthermore, whereas ALX is expressed in unstimulated T cells and its expression remains constant after TCR/CD28 activation (data not shown), the expression of RIBP/TSAd is upregulated after activation (19, 32). In addition, while ALX is actively exported from the nucleus upon T-cell activation (27), a substantial fraction of RIBP/TSAd is localized to the nucleus (16). Examination of ALX/RIBP doubly deficient mice may elucidate the potentially complex interplay between these structurally related signaling adaptors.

ACKNOWLEDGMENTS

The work was supported in part by grant IRG-78-002-26 from the American Cancer Society and by NIH RO1 AI054974 to V.S.S.

We thank David Allman, Avinash Bhandoola, Michael Cancro, Weiguo Zhang, and Mark Shlomchik for reagents and Youhai Chen and Anthony Pajerowski for critical reading of the manuscript. We thank Reka Nagy, Andras Nagy, Janet Rossant, and Wanda Abramow-Newerly for R1 ES cells; Martha Jordan and Gary Koretzky's lab for help with calcium assays; and Jean Richa and the Transgenic and Chimeric Mouse Facility of the University of Pennsylvania.

REFERENCES

1. **Chambers, C. A., and J. P. Allison.** 1997. Co-stimulation in T cell responses. Curr. Opin. Immunol. **9:**396–404.
2. **Chen, C. Y., F. Del Gatto-Konczak, Z. Wu, and M. Karin.** 1998. Stabilization of interleukin-2 mRNA by the c-Jun NH2-terminal kinase pathway. Science **280:**1945–1949.
3. **Choi, Y. B., C. K. Kim, and Y. Yun.** 1999. Lad, an adapter protein interacting with the SH2 domain of p56lck, is required for T cell activation. J. Immunol. **163:**5242–5249.
4. **Dong, C., R. J. Davis, and R. A. Flavell.** 2002. MAP kinases in the immune response. Annu. Rev. Immunol. **20:**55–72.
5. **Espel, E.** 2005. The role of the AU-rich elements of mRNAs in controlling translation. Semin. Cell Dev. Biol. **16:**59–67.
6. **Finco, T. S., T. Kadlecek, W. Zhang, L. E. Samelson, and A. Weiss.** 1998. LAT is required for TCR-mediated activation of PLCgamma1 and the Ras pathway. Immunity **9:**617–626.

7. **Greene, T. A., P. Powell, C. Nzerem, M. J. Shapiro, and V. S. Shapiro.** 2003. Cloning and characterization of ALX, an adaptor downstream of CD28. J. Biol. Chem. **278:**45128–45134.
8. **Hale, K. K., D. Trollinger, M. Rihanek, and C. L. Manthey.** 1999. Differential expression and activation of p38 mitogen-activated protein kinase alpha, beta, gamma and delta in inflammatory cell lineages. J. Immunol. **162:**4246–4252.
9. **Herrin, B. R., A. L. Groeger, and L. B. Justement.** 2005. The adaptor protein HSH2 attenuates apoptosis in response to ligation of the B cell antigen receptor complex on the B lymphoma cell lines, WEHI-231. J. Biol. Chem. **280:**3507–3515.
10. **Herrin, B. R., and L. B. Justement.** 2006. Expression of the adaptor protein Hematopoietic Src Homology 2 is up-regulated in response to stimuli that promote survival and differentiation of B cells. J. Immunol. **176:**4163–4172.
11. **Jain, J., E. Burgeon, T. M. Badalian, P. G. Hogan, and A. Rao.** 1995. A similar DNA-binding motif in NFAT family proteins and the Rel homology domain. J. Biol. Chem. **270:**4138–4145.
12. **Jain, J., C. Loh, and A. Rao.** 1995. Transcriptional regulation of the IL-2 gene. Curr. Opin. Immunol. **7:**333–342.
13. **Kane, L. P., J. Lin, and A. Weiss.** 2002. It's all Rel-ative: NF-kappaB and CD28 costimulation of T-cell activation. Trends Immunol. **23:**413–420.
14. **Kim, J. M., J. M. White, A. S. Shaw, and B. P. Sleckman.** 2005. MAPK p38 alpha is dispensable for lymphocyte development and proliferation. J. Immunol. **174:**1239–1244.
15. **Marti, F., G. G. Garcia, P. E. Lapinski, J. N. MacGregor, and P. D. King.** 2006. Essential role of the T cell-specific adapter protein in the activation of LCK in peripheral T cells. J. Exp. Med. **203:**281–287.
16. **Marti, F., N. H. Post, F. Chan, and P. D. King.** 2001. A transcription function for the T cell-specific adapter (TSAd) protein in T cells: critical role of the TSAd Src homology 2 domain. J. Exp. Med. **193:**1425–1430.
17. **Mulroy, T., and J. Sen.** 2001. p38 map kinase activity modulates alpha beta T cell development. Eur. J. Immunol. **31:**3056–3063.
18. **Oda, T., M. A. Muramatsu, T. Isogai, Y. Masuho, S. Asano, and T. Yamashita.** 2001. HSH2: a novel SH2 domain-containing adapter protein involved in tyrosine kinase signalling in hematopoietic cells. Biochem. Biophys. Res. Commun. **288:**1078–1086.
19. **Rajogopal, K., C. L. Sommers, D. C. Decker, E. O. Mitchell, U. Kortbauer, A. I. Sperling, C. A. Kozak, P. E. Love, and J. A. Bluestone.** 1999. RIBP, a novel Rlk/Txk- and Itk-binding adaptor protein that regulates T cell activation. J. Exp. Med. **190:**1657–1668.
20. **Rincon, M., H. Enslen, J. Raingeaud, M. Recht, T. Zapton, M. S. Su, L. A. Penix, R. J. Davis, and R. A. Flavell.** 1998. Interferon-gamma expression by Th1 effector T cells mediated by the p38 map kinase signaling pathway. EMBO J. **17:**2817–2829.
21. **Rincon, M., and G. Pedraza-Alva.** 2003. JNK and p38 MAP kinases in CD4 and CD8 T cells. Immunol. Rev. **192:**131–142.
22. **Salvador, J. M., M. C. Hollander, A. T. Nguyen, J. B. Kopp, L. Barisoni, J. K. Moore, J. D. Ashwell, and A. J. Fornace.** 2002. Mice lacking the p53-effector gene Gadd45a develop a lupus-like syndrome. Immunity **16:**499–508.
23. **Salvador, J. M., P. R. Mittelstadt, G. I. Belova, A. J. Fornace, and J. D. Ashwell.** 2005. The autoimmune suppressor Gadd45alpha inhibits the T cell alternative p38 activation pathway. Nat. Immunol. **6:**396–402.
24. **Salvador, J. M., P. R. Mittelstadt, T. Guszczynski, T. D. Copeland, H. Yamaguchi, E. Appella, A. J. Fornace, and J. D. Ashwell.** 2005. Alternative p38 activation pathway mediated by T cell receptor-proximal tyrosine kinases. Nat. Immunol. **6:**390–395.
25. **Schuh, K., T. Twardzik, B. Kneitz, J. Heyer, A. Schimpl, and E. Serfling.** 1998. The interleukin 2 receptor alpha chain/CD25 promoter is a target for nuclear factor of activated T cells. J. Exp. Med. **188:**1369–1373.
26. **Schwartz, R. H.** 1997. T cell clonal anergy. Curr. Opin. Immunol. **9:**351–357.
27. **Shapiro, M. J., Y. Y. Chen, and V. S. Shapiro.** 2005. The carboxyl-terminal segment of the adaptor protein ALX directs its nuclear export during T cell activation. J. Biol. Chem. **280:**38242–38246.
28. **Shapiro, M. J., P. Powell, A. Ndubuizu, C. Nzerem, and V. S. Shapiro.** 2004. The ALX Src homology 2 domain is both necessary and sufficient to inhibit T cell receptor/CD28-mediated upregulation of RE/AP. J. Biol. Chem. **279:**40647–40652.
29. **Shapiro, V. S., M. N. Mollenauer, and A. Weiss.** 1998. Nuclear factor of activated T cells and AP-1 are insufficient for IL-2 promoter activation: requirement for CD28 up-regulation of RE/AP. J. Immunol. **161:**6455–6458.
30. **Shapiro, V. S., K. E. Truitt, J. B. Imboden, and A. Weiss.** 1997. CD28 mediates transcriptional upregulation of the interleukin-2 (IL-2) promoter through a composite element containing the CD28RE and NF-IL-2B AP-1 sites. Mol. Cell. Biol. **17:**4051–4058.
31. **Smith, J. L., I. Collins, G. V. Chandramouli, W. G. Butscher, E. Zaitseva, W. J. Freebern, C. M. Haggerty, V. Doseeva, and K. Gardner.** 2003. Targeting combinatorial transcriptional complex assembly at specific modules within the interleukin-2 promoter by the immunosuppressant SB203580. J. Biol. Chem. **278:**41034–41046.
32. **Spurkland, A., J. E. Brinchmann, G. Markussen, F. Pedeutour, E. Munthe, T. Lea, F. Vartdal, and H. C. Aasheim.** 1998. Molecular cloning of a T cell-specific adapter protein (TSAd) containing an Src homology (SH) 2 domain and putative SH3 and phosphotyrosine binding sites. J. Biol. Chem. **273:**4539–4546.
33. **Sugawara, T., T. Moriguchi, E. Nishida, and Y. Takahama.** 1998. Differential roles of ERK and p38 map kinase pathways in positive and negative selection of T lymphocytes. Immunity **9:**565–574.
34. **Umlauf, S. W., B. Beverly, S.-M. Kang, K. Brorson, A.-C. Tran, and R. H. Schwartz.** 1993. Molecular regulation of the IL-2 gene: rheostatic control of the immune system. Immunol. Rev. **133:**177–197.
35. **Ward, S. G., R. V. Parry, J. Matthews, and L. O'Neill.** 1997. A p38 map kinase inhibitor SB203580 inhibits CD28-dependent T cell proliferation and IL-2 production. Biochem. Soc. Trans. **25:**304S.
36. **Wu, C.-C., S.-C. Hsu, H.-M. Shih, and M.-Z. Lai.** 2003. Nuclear factor of activated T cells c is a target of p38 mitogen-activated protein kinase in T cells. Mol. Cell. Biol. **23:**6442–6454.
37. **Wu, L. W., L. D. Mayo, J. D. Dunbar, K. M. Kessler, O. N. Ozes, R. S. Warren, and D. B. Donner.** 2000. VRAP is an adaptor protein that binds KDR, a receptor for vascular endothelial cell growth. J. Biol. Chem. **275:**6059–6062.
38. **Zhang, J., K. V. Salojin, J. X. Gao, M. J. Cameron, I. Bergerot, and T. L. Delovitch.** 1999. p38 mitogen-activated protein kinase mediates signal integration of TCR/CD28 costimulation in primary murine T cells. J. Immunol. **162:**3819–3829.
39. **Zhang, W., C. L. Sommers, D. N. Burshtyn, C. C. Stebbins, J. B. DeJarnette, R. P. Trible, A. Grinberg, H. C. Tsay, H. M. Jacobs, C. M. Kessler, E. O. Long, P. E. Love, and L. E. Samelson.** 1999. Essential role of LAT in T cell development. Immunity **10:**323–332.
40. **Zhu, M., O. Granillo, R. Wen, K. Yang, K. Dai, D. Wang, and W. Zhang.** 2005. Negative regulation of lymphocyte activation by the adaptor protein LAX. J. Immunol. **174:**5612–5619.
41. **Zhu, M., E. Janssen, K. Leung, and W. Zhang.** 2002. Molecular cloning of a novel gene encoding a membrane-associated adaptor protein (LAX) in lymphocyte signaling. J. Biol. Chem. **277:**46151–46158.